ISSN 0208-7774 TRIBOLOGIA 3/2017 p. 127–136

Andrzej RYNIEWICZ[*], Anna M. RYNIEWICZ[**]

IDENTIFICATION OF FRICTION CONDITIONS IN HUMAN JOINTS

IDENTYFIKACJA WARUNKÓW TARCIA W STAWACH CZŁOWIEKA

Key words: biobearing, structural and anatomical identification, biomechanics, BEHL.

Abstract

The purpose of the paper is to explain the friction conditions and the lubrication mechanism in healthy joints, based on rheological tests of synovial fluid and the identification of structures and the shape of articular surfaces. The tests were performed on cadaver preparations of large lower limp joints: hip, knee, and ankle joints. The analysis included combined experimental activities with the use of modern research and test techniques in the area of viscosity and microscopy as well as diagnostic imaging, image analysis, modelling, and FEM simulation. The tests performed allowed for the analysis of lubrication process which can be described as bioelastohydrodynamic lubrication (BEHL). The most important are viscoelasticity properties of the synovial fluid and the process whereby the external load is taken over by the pressure generated by a set of oil wedges of synovial fluid formed by naturally wavy articular surface. The multi-layer structure of the joints is characterised by variable wavy shape of cartilaginous surfaces and of bone tissue and by the variable wavy thickness of the cartilage.

Słowa kluczowe: biołożysko, identyfikacja strukturalna i anatomiczna, modelowanie, biomechanika, BEHL.

Streszczenie

Celem opracowania jest wyjaśnienie warunków tarcia i mechanizmu smarowania w stawach prawidłowych na podstawie badań reologicznych cieczy synowialnej i identyfikacji struktur oraz kształtu powierzchni stawowych. Materiałem badań były stawy z preparatów kadawerskich. Badano duże stawy kończyny dolnej: biodrowe, kolanowe i skokowe górne. Analiza obejmowała skojarzone działania eksperymentalne z wykorzystaniem nowoczesnych technik badawczych w obszarze lepkości i mikroskopii oraz diagnostyki obrazowej, analizy obrazu, modelowania i symulacji numerycznej MES. Przeprowadzone badania pozwoliły na analizę procesu smarowania, który może być określony bioelastohydrodynamicznym smarowaniem (BEHL). Dominujące znaczenie mają lepkosprężyste właściwości mazi stawowej oraz proces polegający na przejęciu obciążenia zewnętrznego przez ciśnienie generowane w układzie klinów smarnych wypełnionych mazią a utworzonych przez anatomicznie pofalowane powierzchnie stawowe. W wielowarstwowej budowie stawów występuje falista zmiana kształtu powierzchni chrzęstnych, falista zmiana kształtu powierzchni kostnych oraz falista zmiana grubości tkanki chrzęstnej.

INTRODUCTION

Human joints are structures optimally designed for their biomechanical functions and biotribological processes **[L. 1–4]**. They may serve as a model for technical solutions; unfortunately, in our present state of knowledge, the comprehensive replication of phenomena and processes taking place there is not possible **[L. 5–8]**.

The purpose of the paper is to explain the friction conditions and the lubrication mechanism in normal (healthy) joints, based on rheological tests of synovial fluid as well as the identification of structures and the shape of the articular surfaces. The analysis covered combined experimental activities with the use of modern research techniques, modelling, and FEM simulation.

MATERIAL AND METHOD

The materials used in the research work, upon consent of the Boards of Bioethics, were joints obtained from cadaver preparations, aged between 30-40 years. The

[*] Cracow University of Technology, Faculty of Mechanical Engineering, Laboratory of Coordinate Metrology, al. Jana Pawła II 37, 31-864 Kraków, Poland.

[**] AGH University of Science and Technology, Faculty of Mechanical Engineering and Robotics, al. A. Mickiewicza 30, 30-059 Kraków, Poland.

tests covered hip, knee, and ankle joints. 10 joints of each type were selected **[L. 9, 10]**. No pathological abnormalities were observed in the selected joints that were indicative of any disease.

The method comprised the following procedures:

- Rheological tests of synovial fluid, with the use of Anton Paar oscillatory rheometer;
- Tests of surface layer of articular cartilage, with the use of atomic force microscope (AFM) and scanning electron microscope (SEM) (IOEL 5400 electron microscope fitted with an energy dispersive spectrometer (EDS));
- Diagnostic imaging by means of computed tomography (CT), using spiral 64-slices CT scanner Siemens Somatom Cardiac;
- Diagnostic imaging with the use of magnetic resonance (MR) – Magneton Sonata Maestro Class;
- An analysis of CT and MR images, preparation of 3-D models of the investigated joints;
- The determination of the shape of articular surfaces, using a coordinate measuring machine Leitz PMM 12106; and,
- Modelling and simulation tests with the use of MES.

The paper presents only some of the tests performed. However, they seem sufficient to prove the thesis that the lubrication mechanisms observable in joints are based on the interaction of articular structures perfectly designed at a nano, micro, and macro level to perform their functions.

TESTS RESULTS AND DISCUSSION

Synovial fluid plays a major role in biotribology and physiology of joints. It is a medium lubricating the interacting surfaces, delivering nutrients to articular cartilage, and absorbing redundant metabolites. In normal conditions, articular cavity contains a small amount of fluid. In large human joints, there is, on average, 0.5 ml to 3 ml of synovial fluid. Rheological tests of synovial fluid included rotation and oscillation tests. The tests concerning Taylor-Couette flow in a fissure between the rotating cone and the plate were carried out in isothermal conditions, using a state-of-the-art rotational rheometer Physica MCR 501 manufactured by Anton Paar. Fluid samples were taken from the joints, using a puncture syringe, directly before the tests. Rotational measuring was used to produce flow and viscosity curves of the synovial fluid and of a joint preparation used in visco-supplementation **(Fig. 1) [L. 5]**.

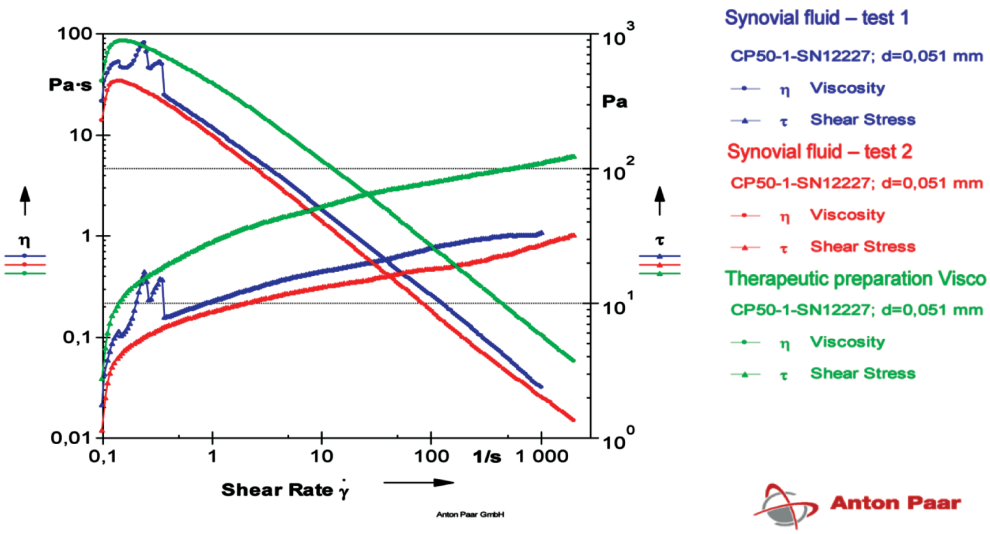

Fig. 1. Flow and structural viscosity curves for synovial fluid and Visco fluid [L. 5]
Rys. 1. Zestawienie krzywych płynięcia i krzywych lepkości strukturalnej mazi stawowej oraz płynu Visco **[L. 5]**

The curves produced show that the synovial joint fluid and Visco preparation are non-Newtonian shear-thinning liquids. Fluid parameters measured at a temperature of 36.6°C are, to a considerable degree, dependent on the shear rate and vary within a broad range. Articular fluid viscosity at the shear rate of 0.1 s^{-1} equalled 21 Pa·s and 15 Pa·s, while at shear rate of 1000 s^{-1} – 0.03 Pa·s and 0.018 Pa·s. Joint preparation viscosity at the shear rate of 0.1s^{-1} equalled 35 Pa·s, while at shear rate of 1000 s^{-1} – 0.1 Pa·s. Decrease of structural viscosity characteristic for synovial fluid is dependent upon its chemical structure and spatial configuration of the hyaluronic acid and protein complex. Hyaluronic acid is a saccharide biopolymer with a molecular mass of 500–700 kD. It determines the viscoelasticity properties of synovial fluid and cartilaginous tissue. In complex compounds with proteoglycans and proteins, it serves as a mechanic buffer protecting chondrocytes against damage. The test findings are confirmed in literature on the subject **[L. 11–14]**. In order to determine the

viscosity properties of the synovial fluid oscillatory tests were performed, consisting in subjecting samples to sinusoidal varying stress or straining and in recording the reactions. The following parameters were measured during the tests: storage modulus G' and loss modulus G'' as well as synovial fluid complex viscosity η^*. G' modulus represents the amount of energy stored by the sample and flexibility parameters, while G'' modulus is related to the energy dispersion and reflects viscosity parameters of the synovial fluid. The shorter the straining time (in other words the faster the straining), the more distinctive were the elasticity properties of the synovial fluid **(Fig. 2) [L. 5]**. Diagrams showing the G' and G'' dependency on oscillation frequency can provide information on changes taking place in the fluid structure and, particularly, in its tribological properties. Increasing values of storage modulus G' in the synovial fluid and in the visco-supplementation fluid are the evidence that elastic gel structures are formed there. Normal stresses push away the interacting surfaces and prevent any contact between them.

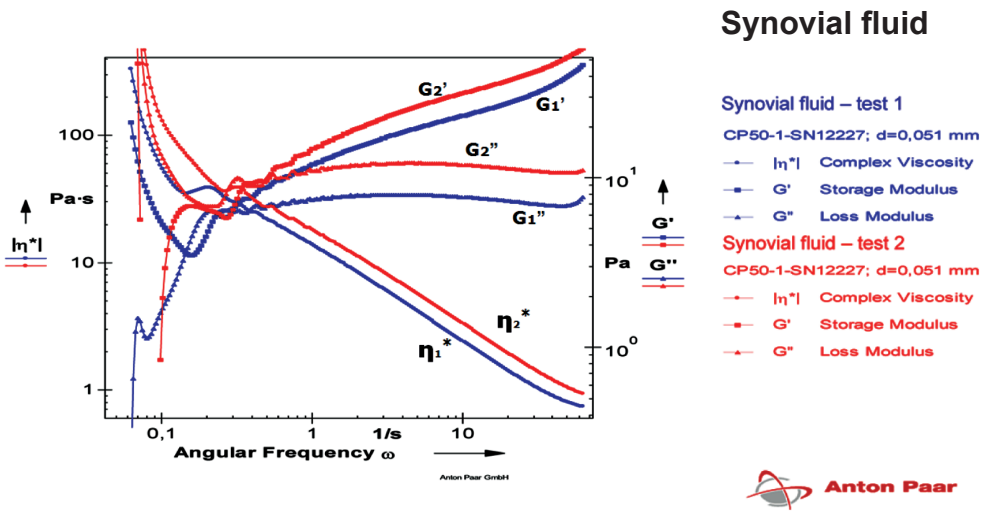

Fig. 2. Rheological oscillatory measurements at variable frequencies and constant strain [L. 5]
Rys. 2. Reologiczne pomiary oscylacyjne przy zmiennej częstotliwości i stałym odkształceniu **[L. 5]**

Oscillatory measurements of synovial fluid demonstrated the major importance of viscoelasticity. Its presence in a node, even at very mild extortion, generated normal stresses, which were perpendicular to the affected surface. They were caused by the elastic deformation of fluid particles under compression and movements within the testing node.

In order to assess the morphology of interacting surfaces, the surface layer of the hyaline cartilage taken from articular surfaces of the investigated joints and the fibrocartilage forming the knee joint menisci were examined, using AFM **(Fig. 3) [L. 15]**. The presented stereometric image of the fibrocartilage from the knee joint meniscus was representative for other cartilaginous structures involved in tribological interaction. It formed a regular and homogeneous pattern of waves. The maximum height of roughness S_y varied between 235 and 420 nm, and the arithmetic mean deviation of the roughness profile from the mean line S_a was between 29 nm and 68 nm, while the mean square deviation of the surface S_q (RMS) was between 32 nm and 75 nm.

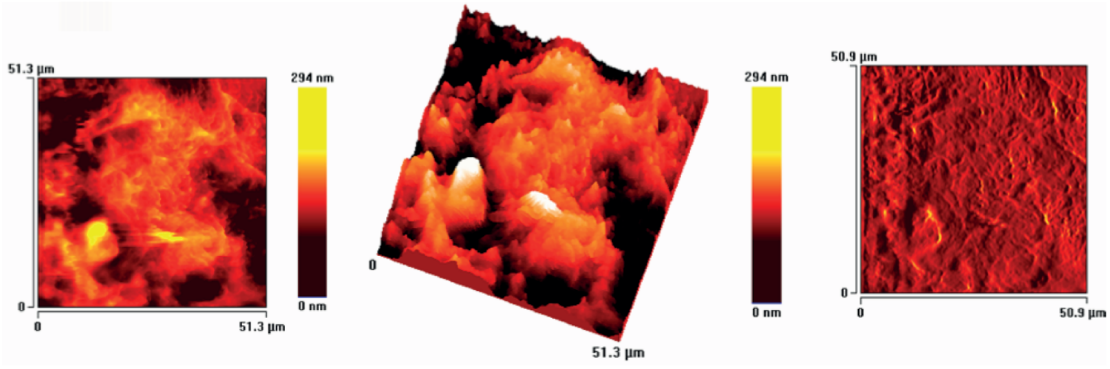

Fig. 3. An example of stereometric image of the surface layer of the fibrous cartilage (meniscus) from a knee joint – AFM [L. 15]
Rys. 3. Przykładowy obraz stereometryczny warstwy wierzchniej chrząstki włóknistej (łąkotka) ze stawu kolanowego – badanie AFM **[L. 15]**

Subsequently, the cross-sections of articular hyaline cartilage were examined. The analyses were performed in two stages on samples taken from various areas. The cross-sections clearly showed cartilage tissue established on bone tissue **(Fig. 4)**. In all areas, the thickness of cartilage tissue varied, depending on the location of the articular surface **[L. 6, 16]**. Involved in the lubrication process is the wavy surface layer of the articular cartilage. It is very smooth, which is evidenced by the roughness parameters determined during the tests. Collagen fibres forming arcades and embedded in the cartilage matrix make the surface layer mildly wavy, regular, and not oriented in any specific direction **(Fig. 5)**. This was confirmed by AFM and scanning tests as well as the tests performed with the use of confocal microscope.

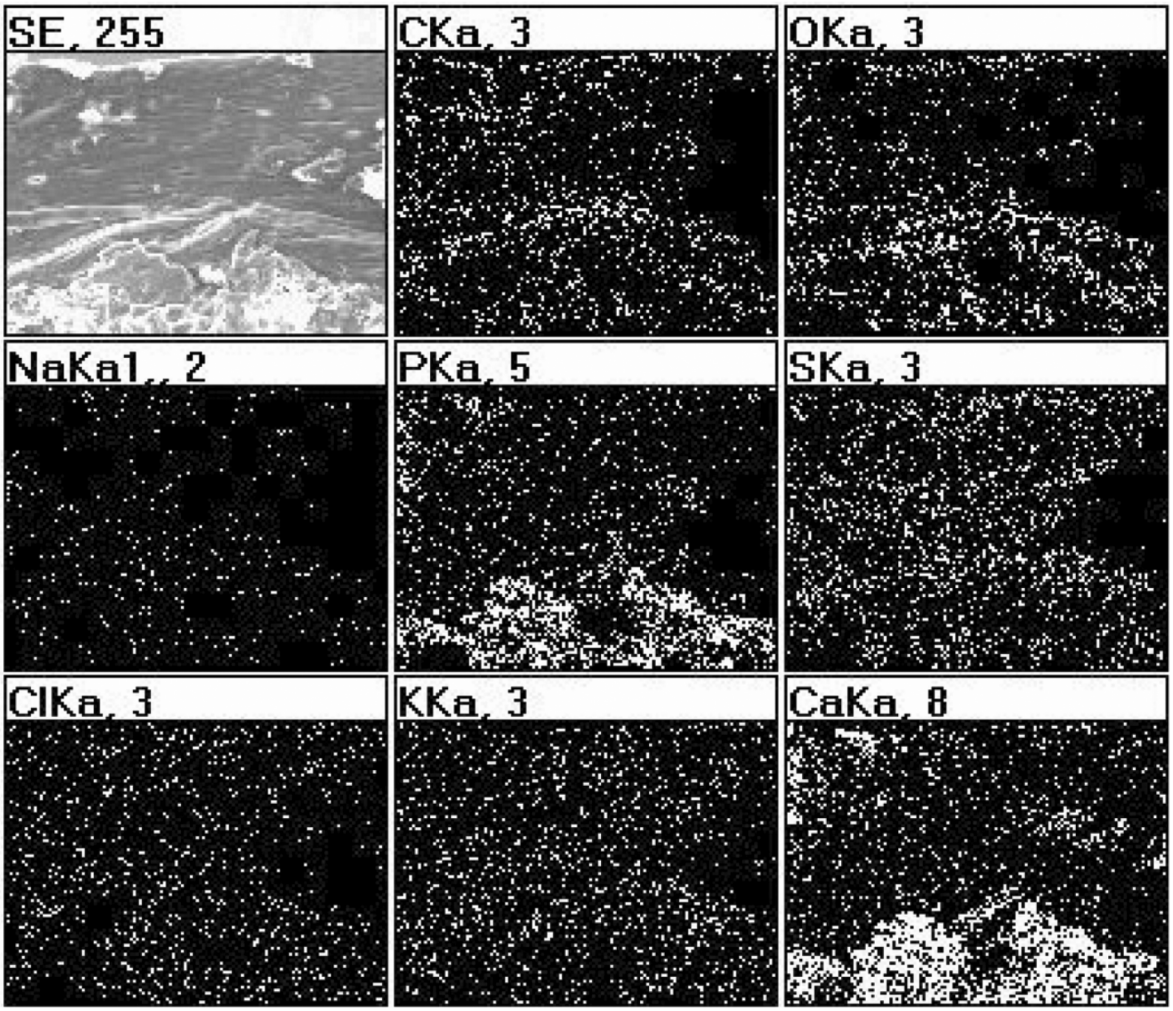

Fig. 4. Cross-section of articular hyaline cartilage and calcified bone structure – SEM image and element analysis
Rys. 4. Przekrój przez szklistą chrząstkę stawową i zwapniałą strukturę kostną – obraz SEM wraz z analizą pierwiastkową

Assessment of joint lubrication mechanisms was possible after identifying macro-shapes of joint elements and of the distribution of cartilage thickness across articular surfaces. The parameters were determined for knee, hip **(Figs. 6** and **7)** and ankle joints through the tests performed on cadaver preparations using a coordinate measuring machine **[L. 5, 17]**.

The shape of the head of femur **(Fig. 6)** and of the hip joint acetabulum **(Fig. 7)** identified in the course research work was presented. The research findings included the analysis of the shape of normal (healthy) joint and the shape of the joint affected by maceration of cartilage. Important information obtained from the measurements taken was the distribution of points with positive and negative form deviations.

Based on the form deviation measurements of sphericity of the head and acetabulum of the hip joint, the areas of positive and negative form deviations could be identified. Regarding the femur head, the deviations were observed interchangeably in four areas of similar size, distributed symmetrically to the axis of the neck of femur. Regarding the lunate surface of the acetabulum,

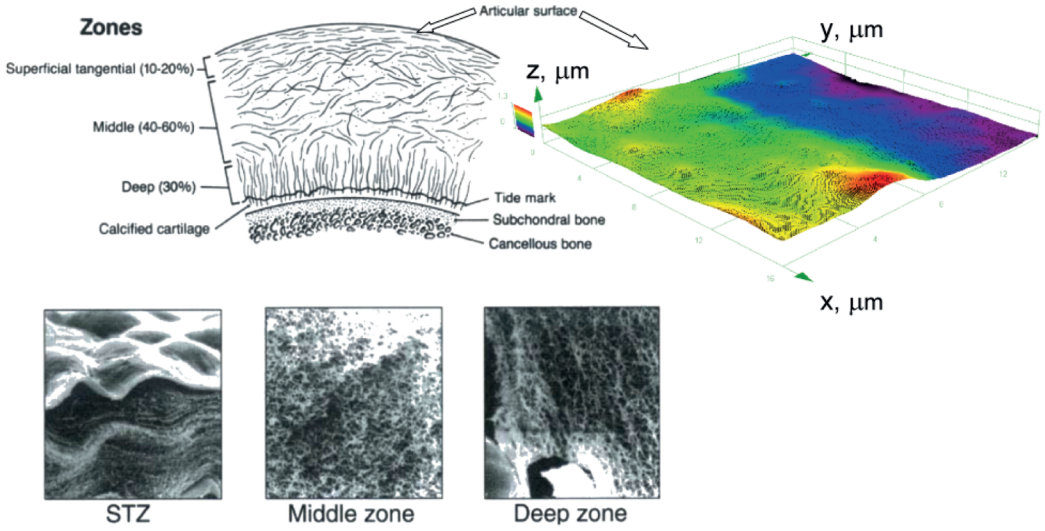

Fig. 5. Geometric structure of the surface layer of the articular hyaline cartilage from confocal microscope and areas marked schematically in cross section

Rys. 5. Struktura geometryczna warstwy wierzchniej chrząstki szklistej w mikroskopie konfokalnym oraz schematycznie zaznaczone strefy w przekroju poprzecznym

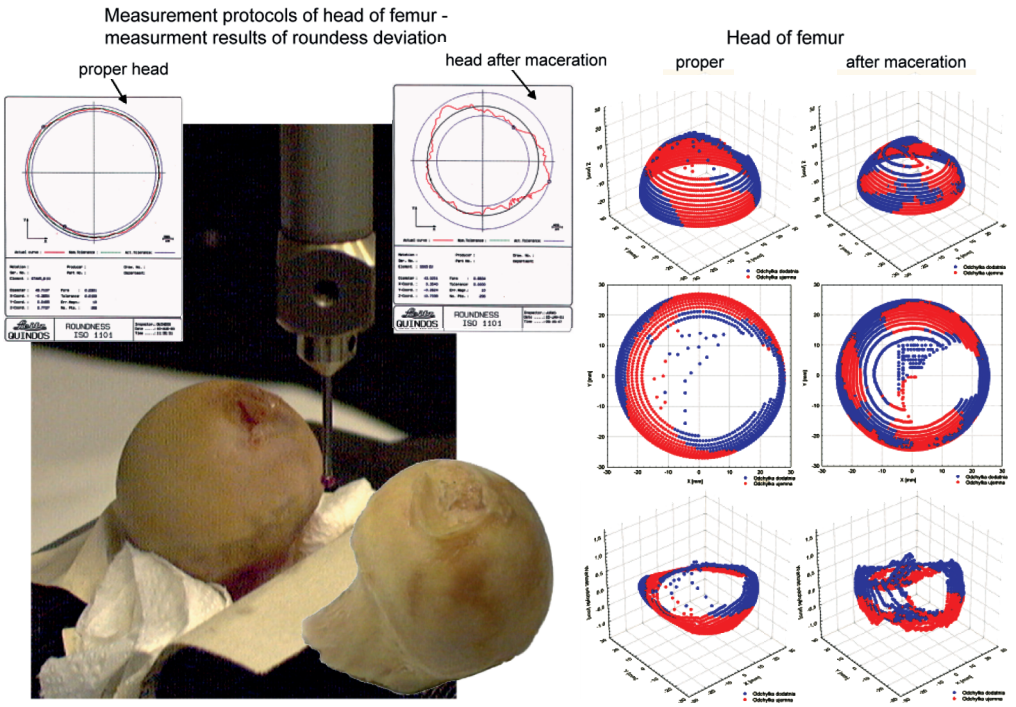

Fig. 6. Examination, using coordinate measuring machine, of the femur head (m. l. 40 b.p.) covered with normal cartilage and of the head affected by cartilage maceration: a) procedure; b), c) shape measurement results – distribution of measurement points with + and – deviations marked (3D and 2D); d) form deviation values at individual measurement points [L. 4]

Rys. 6. Badanie na WMP kształtu głowy kości udowej (m. l. 40 b.p.) pokrytej prawidłową tkanką chrzęstną oraz głowy po maceracji chrząstki: a) procedura badawcza; b), c) wyniki pomiarów kształtu – rozmieszczenie punktów pomiarowych z oznaczeniem odchyłek + i – (układ 3D i 2D); d) wartości odchyłek kształtu w poszczególnych punktach pomiarowych **[L. 4]**

the areas of positive and negative deviations were distributed annularly, but they were shifted relative to one another. Human articular surfaces in hip joints having the shape described above were characterised by variable wavy thickness of the fissure at motion relative to any axis. On the femur head and acetabulum, directly beneath the cartilage layer, there was a layer of calcified bone. Investigation of form divinations of the bone layer

of the femur and of the lunate surface of the acetabulum also showed areas with positive and negative deviations. In both cases, the areas were annularly distributed and shifted relative to one another. In the femur head, the thickness of cartilage was between 0.9 mm and 2.1 mm, with a characteristic distribution of the cartilage in the femur head, similar in all investigated joints. In the acetabulum, the cartilage was between 0.5 mm and 2.1 mm thick, and the determined cartilage distribution pattern was typical of the investigated joints **[L. 12, 14, 15, 17, 19]**.

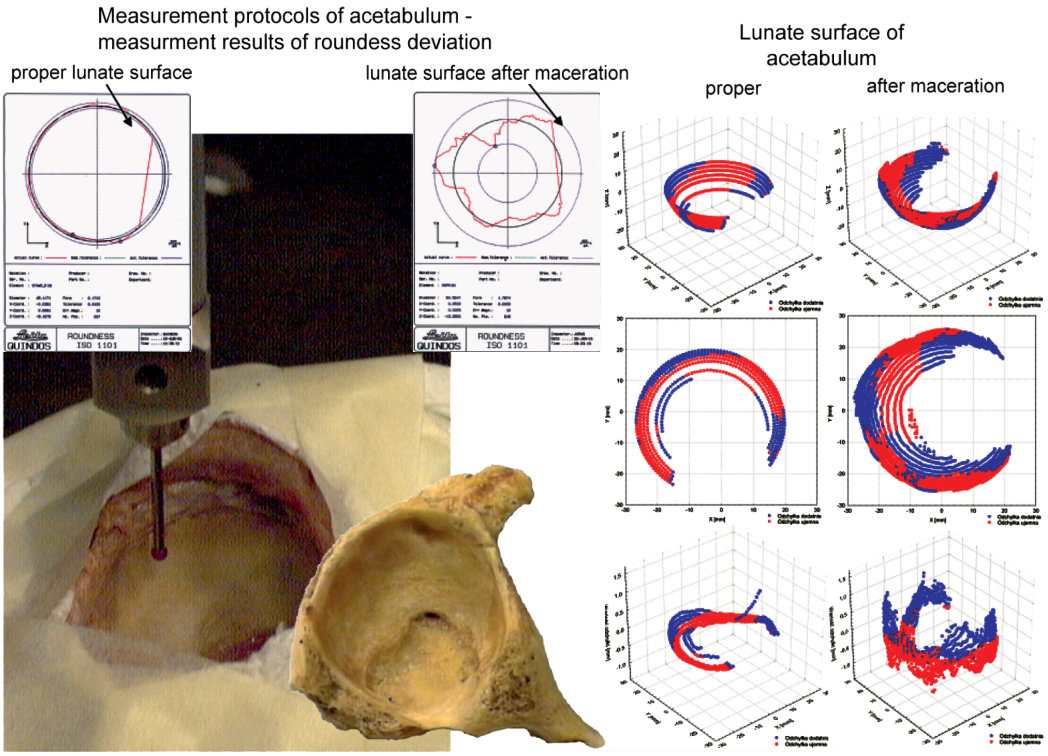

Fig. 7. Examination, using coordinate measuring machine, of the shape of normal hip joint acetabulum (m. l. 40 b.p.) covered with normal cartilage and of the acetabulum affected by cartilage maceration: a) procedure; b), c) shape measurement results – distribution of measurement points with + and – deviations marked (3D and 2D); d) form deviation values at individual measurement points [L. 4]

Rys. 7. Badanie na WMP kształtu prawidłowej panewki stawu biodrowego (m. l. 40 b.p.) pokrytej chrząstką oraz panewki po maceracji chrząstki: a) procedura badawcza; b), c) wyniki pomiarów kształtu – rozmieszczenie punktów pomiarowych z oznaczeniem odchyłek + i – (układ 3D i 2D); d) wartości odchyłek kształtu w poszczególnych punktach pomiarowych **[L. 4]**

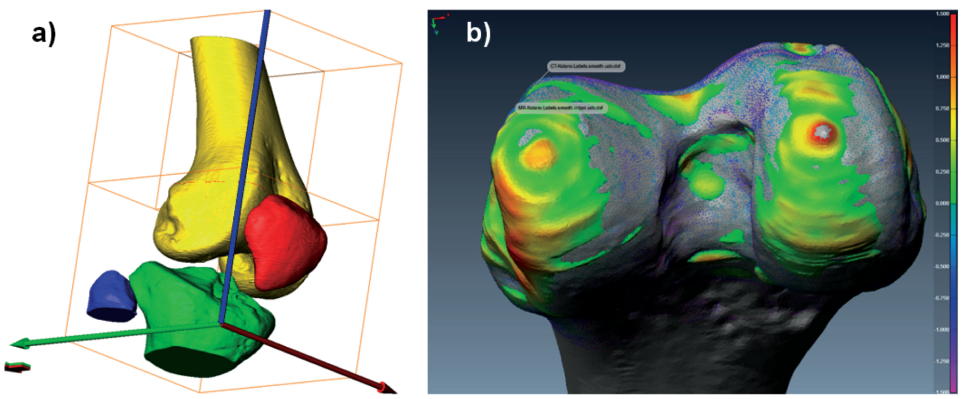

Fig. 8. Reconstruction of normal structure of a knee joint (m. preparation No. 1717): a) based on CT, b) based on combined CT and MR images [L. 5, 17]

Rys. 8. Rekonstrukcja prawidłowych struktur stawu kolanowego (m.preparat nr 1717): a) na podstawie CT, b) na podstawie fuzji obrazów CT i MR **[L. 5, 17]**

The identified shapes of the articular surfaces of the hip joint are indicative of the characteristic wavy shape of the femur head surface and the characteristic wavy shape of the lunate surface of the acetabulum as well as the characteristic variable thickness distribution of cartilage on these surfaces. This anatomic structure of normal articular surfaces is the key factor causing the lack of congruence in interaction and the formation of oil wedges which, in physiological conditions, are filled with synovial fluid. When confronted with the literature on the subject, this particular form of articular macro-surfaces and irregular thickness distribution of cartilage on these surfaces has turned out to be a completely new research problem.

In order to assess the shape and lubrication mechanism of the joints, a procedural algorithm was developed, using CT and MR diagnostic imaging for the purpose of virtual reconstruction of the joints, modelling, and a simulation of stresses, displacements, and strains during locomotive actions. After diagnostic imaging, the images and scans were analysed, using Amira 5.2.2 and Geomagic Qualify 12 applications. Spatial mapping of bone and cartilage structures of the investigated knee joint were presented **(Fig. 8) [L. 16, 19–22]**. Using the software developed for that purpose, transformation to FEMAP NE/Nastran v.8.3 Modeler application was performed. Boundary conditions and endurance parameters were set for the generated numerical models and biomechanical analyses were performed.

The conditions in which loads are transferred were analysed on the basis of the modelled object of research **(Fig. 9)**.

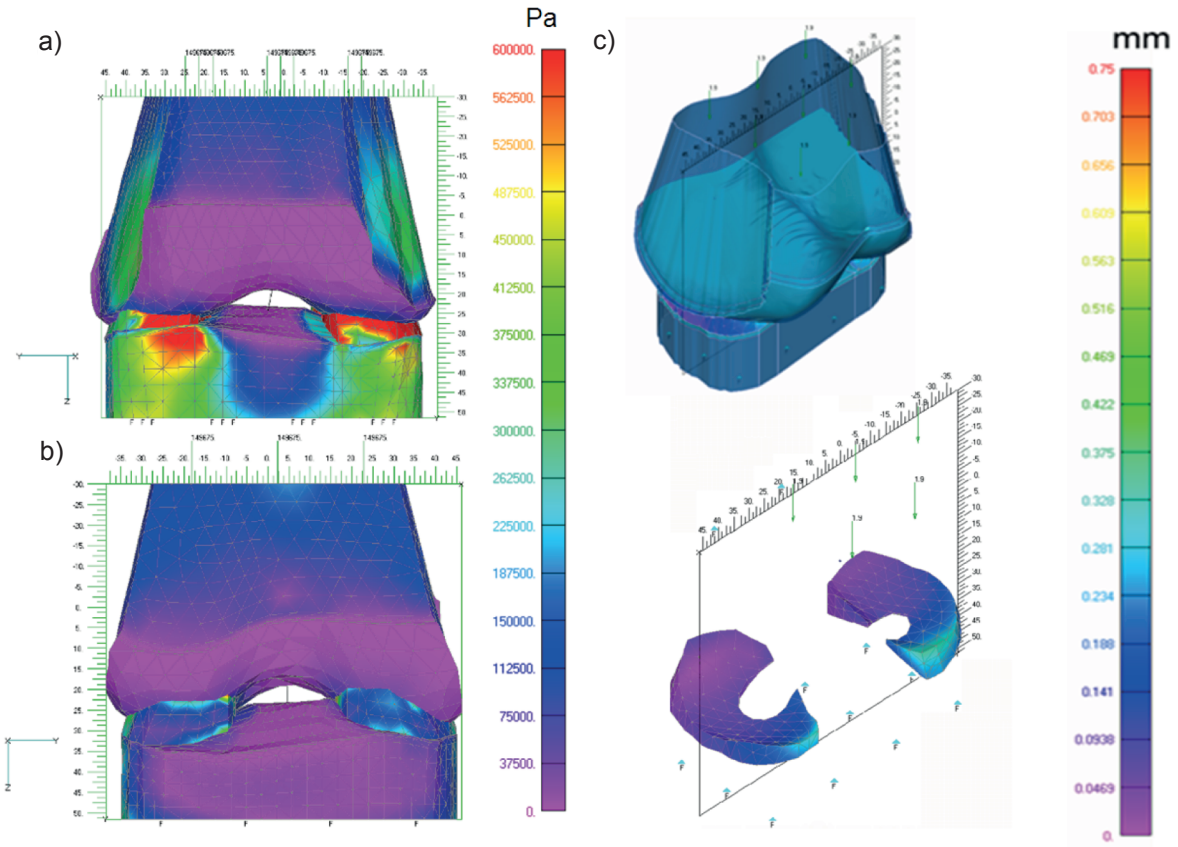

Fig. 9. Numerical simulations of the model of normal knee joint obtained by means of combining CT and MR images (m. preparation No. 1717): a) distribution of stresses – front view, b) distribution of stresses – rear view, c) distribution of dislocations in menisci isolated from the research model

Rys. 9. Symulacje numeryczne w modelu prawidłowego stawu kolanowego utworzonego przez fuzję obrazów CT i MR (m. preparat nr 1717): a) rozkład naprężeń w widoku z przodu, b) rozkład naprężeń w widoku z tyłu, c) rozkład przemieszczeń w łąkotkach wyizolowanych z modelu badawczego

Reduced stresses varied in the knee joint structure with the maximum values reaching 7 MPa. The maximum stresses were observed in menisci and under-cartilage areas of the tibia, between 6 MPa and 7 MPa, and of femur – between 4.5 MPa to 5 MPa. Clear diversification of stresses between the cartilage and bone tissue were observed in the femur and tibia. The stress values in cartilage structures were much lower, ranging

from 1.5 MPa to 1.8 MPa, than in bone structures, both in the contact area and elsewhere. Minimum stress was observable in the intercondylar area of the femur and on the intercondylar eminence. Low stress areas were observable near ligaments. Assessment of displacement distribution suggests an amortisation function of the menisci **(Fig. 9c)**. Displacements on femur and tibia condyles are suppressed in the contact with menisci and differ in the meniscus structure. Higher displacement values are observed in medial meniscus, while lower values were observed in the lateral one. Simulation of displacements in meniscus structures demonstrated displacements in the anterior section of between 0.18 mm and 0.35 mm, and in posterior section – between 0 and 0.1 mm.

Regarding the ankle joint, the tribological function of the lubricating fold formed by the tibiofibular syndesmosis fibres should be mentioned **(Fig. 10)**. Very important for the lubrication analysis of that joint are the movements of the fibula in connection with the structures of fibrous membrane of the tibiofibular syndesmosis and synovial fold, which ensure the transport of the fluid from the forked opening area in the upper articular surface. The load exerted on this surface is reduced in the synovial fold area, which is suggested by the stress analysis; however, stress simulation **[L. 5]** showed that the surface is subject to considerable displacements.

The layered wavy structure of the articular surfaces at nano, micro, and macro level enables optimum performance of the function consisting in the transfer of external loads in elastic contact in the presence of oil bio-wedges. At the same time, it enables the performance of physiological processes in tissues. Synovial fluid generated as a serum transudate in the synovial membrane is transported, in the specific volume, to the articular cavity. Being under pressure and stimulated by the presence of oil wedges in the normal joints causes separation and lubrication of interacting cartilage layers. In addition, through the diffusion process, it penetrates into cartilage structure, keeps it in a state of elastic saturation, regenerates collagen fibres, and – most importantly – nourishes the cartilage cells – chondrocytes. Hydrostatic pressure of water bounded with proteoglycans present in the collagen structure makes the cartilage durable and resistant to loads/strains.

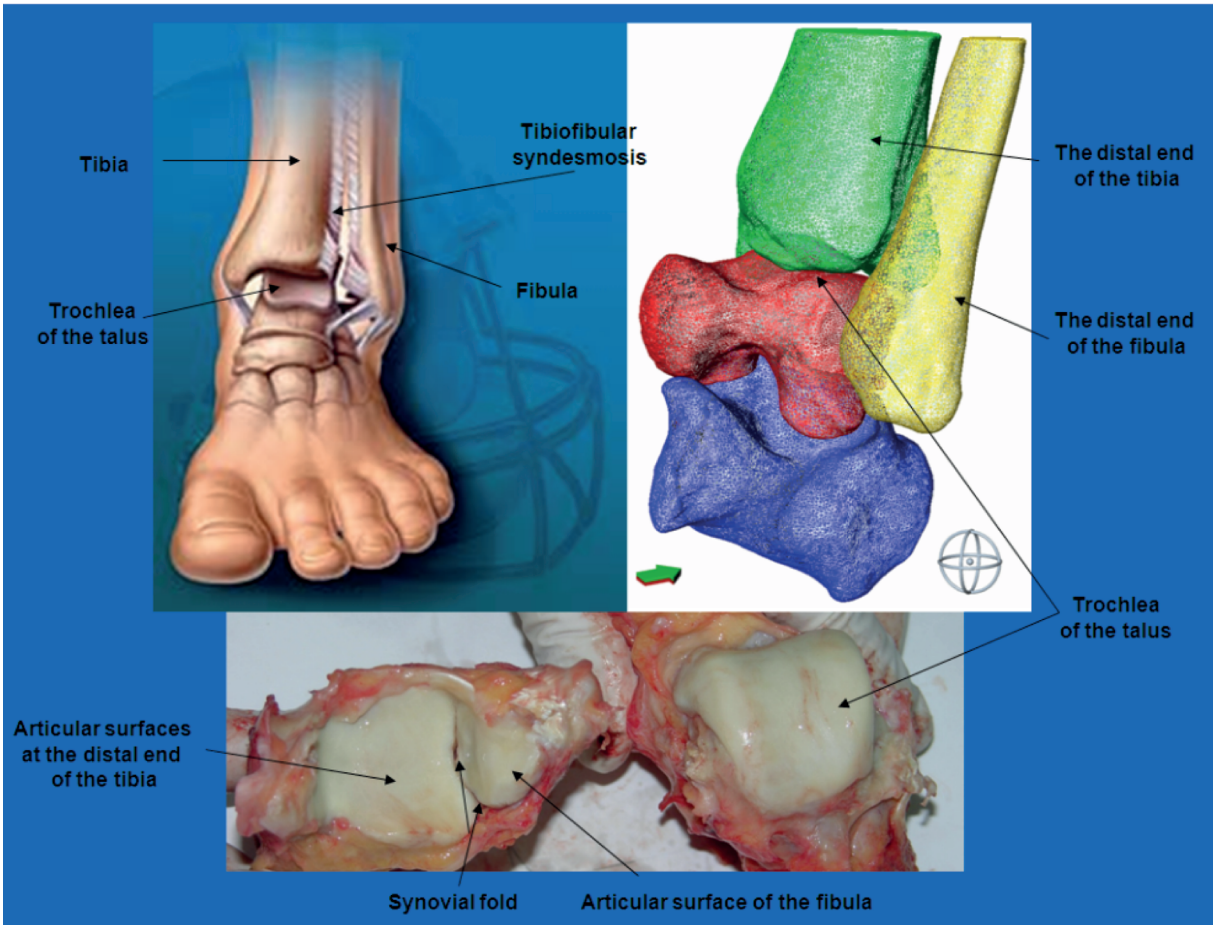

Fig. 10. Anatomic structures facilitating the process of lubrication of the ankle joint
Rys. 10. Struktury anatomiczne wspomagające proces smarowania stawu skokowego górnego

CONCLUSIONS

Investigation of articular structures in large joints of the lower limb enabled the analysis of the lubrication process that can be described as bioelastohydrodynamic lubrication (BEHL) and substantially differs from other mechanisms discussed in technical tribology.

The following two phenomena play the dominant role:

1. The phenomenon is dependent upon the structural and biochemical properties of the synovial fluid, characterised by strain hardening combined with the presence of normal stresses. Experiments and tests demonstrated that the process is specific to articular structures.
2. The effect resulting from the geometry of the friction pair is that the load is taken over by the pressure generated by a set of oil wedges of synovial fluid formed by naturally wavy working surfaces. Due to the shapes of articular surfaces, there are fissures which, when strain is exerted or locomotive action is performed, are not symmetrical relative to the rotation axis, and the location of the instantaneous centre of rotation is variable.

The multi-layer structure of the joints is characterised by the variable wavy shape of cartilaginous surfaces and of bone tissue and by the variable wavy thickness of the cartilage. The structure and the optimum endurance parameters of the layers affect the lubrication mechanism. The analysis of strains, displacements, and stresses in biobearing confirms that the cartilage forming the articular surfaces and tribological auxiliary structures play an active role in the lubrication. Stresses amortised in the cartilage are transferred into the bone structures which are stronger and biologically designed to remodelling when load is exerted. The phenomenon of taking over the load by internal structures was observed in all analysed joints. It can be concluded that the shape as well as anatomical and physiological multi-layer structure of a joint ensures resistance to external forces.

REFERENCES

1. Choudhury D., Ghosh S., Ali F., Vrbka M., Hartl M., Krupka I.: The Influence of Surface Modification on Friction and Lubrication Mechanism Under a Bovine Serum–Lubricated Condition. Tribology Transactions, 59, 2, 2016, 316–322.
2. Li F., Wang A., Wang C.: Analysis of friction between articular cartilage and polyvinyl alcohol hydrogel artificial cartilage. Journal of Materials Science: Materials in Medicine, 27, 5, 2016, 1–8.
3. Moore A.C., Burris D.L.: Tribological rehydration of cartilage and its potential role in preserving joint health. Osteoarthritis and Cartilage, 25, 1, 2017, 99–107.
4. Tian Q., Lou J., Mikkola A.: A new elastohydrodynamic lubricated spherical joint model for rigid-flexible multibody dynamics. Mechanism and Machine Theory, 107, 2017, 210–228.
5. Ryniewicz A.M.: Identification, modelling and biotribology of human joints, AGH University of Science and Technology Press, Kraków 2011.
6. Ryniewicz A.M.: Analysis of the lubrication mechanism of the human hip joint. Monograph No. 111, UWND AGH, Kraków 2002.
7. Murakami T., Yarimitsu S., Sakai N., Nakashima K., Yamaguchi T., Sawae, Y.: Importance of Adaptive Multimode Lubrication Mechanism in Natural Synovial Joints. Tribology International, 2016.
8. Singh N.: Synovial Joints and Lubrication mechanisms. International Journal of Computational and Applied Mathematics, 12, 1, 2017, 29–33.
9. Opinion No. 146 KBL/OIL/2003 of the 11th of June 2003, the Bioethics Committee of the District Medical Chamber in Cracow.
10. Opinion No. 146 KBET/434/B/2003 of 29 May 2003 of the Bioethics Commission of the Jagiellonian University.
11. Jahn S., Seror J., Klein J.: Lubrication of articular cartilage. Annual Review of Biomedical Engineering, 18, 2016, 235–258.
12. Ermakov S., Beletskii A., Eismont O., Nikolaev V.: Modern Concepts of Friction, Wear and Lubrication of Joints. In Liquid Crystals in Biotribology Springer International Publishing, 2016, 99–121.
13. Ermakov S., Beletskii A., Eismont O., Nikolaev V.: Effect of Liquid Crystals on Biological Mechanisms of Reducing Joint Friction. In Liquid Crystals in Biotribology. Springer International Publishing, 2016, 123–166.
14. Wu Y., Ferguson S.J.: The influence of cartilage surface topography on fluid flow in the intra-articular gap. Computer Methods in Biomechanics and Biomedical Engineering, 2016, 1–10.
15. Ryniewicz A.M., Ryniewicz A., Lekka M.: The analysis of surface layer of the articular cartilage using modern microscopic techniques, Przegląd Lekarski, 64, 2007, 140–146.

16. Andreisek G., Weiger M.: T2* mapping of articular cartilage: current status of research and first clinical applications. Invest Radiol., 49, 1, 2014, 57–62.
17. Ryniewicz A.: Accuracy assessment of biobearings elements shape mapping in in vivo and in vitro analysis, Publishing House of the Warsaw University of Technology, Warszawa 2013.
18. Tuan R.S., Korkusuz F. : Joint Cartilage. In Musculoskeletal Research and Basic Science. Springer International Publishing, 2016, 367–386.
19. Orozco L., Munar A., Soler R., Alberca M., Soler F., Huguet M., Sentis J., Sanches A., García-Sancho J.: Treatment of knee osteoarthritis with autologous mesenchymal stem cells: a pilot study, Transplantation, 95, 12, 2013, 1535–1541.
20. Camp C.L., Stuart M.J., Krych A.J., Levy B.A., Bond J.R., Collins M.S., Dahm D.L.: CT and MRI measurements of tibial tubercle–trochlear groove distances are not equivalent in patients with patellar instability, The American journal of sports medicine, 41, 8, 2013, 1835–1840.
21. Rodriguez-Merchan E., Regeneration of articular cartilage of the knee: basic concepts, Articular Cartilage Defects of the Knee, Wydawnictwo Springer-Verlag, Italia 2012, 1–16.
22. Windt T.D., Welsch G.H., Brittberg M., Vonk L.A., Marlovits S., Trattnig S., Saris D.B.F.: Is magnetic resonance imaging reliable in predicting clinical outcome after articular cartilage repair of the knee? American journal of sports medicine, 41, 7, 2013, 1695–1702.